Journal of Thermal Analysis and Calorimetry, Vol. 73 (2003) 127–142

PREHISTORIC TERRACOTTAS FROM THE LIBYAN TADRART ACACUS
Thermoanalytical study and characterization

L. Campanella, G. Favero, P. Flamini and M. Tomassetti[*]

Dipartimento di Chimica, Universitá di Roma 'La Sapienza', Piazza A. Moro 5, 00185 Roma, Italy

(Received May 3, 2002; in revised form November 2, 2003)

Abstract

The specimens studied in the present work consist of five terracotta fragments from an archaeological dig on the Libyan Tadrart Acacus massif, dating back to about 5000–8000 B.C.

The specimens were analysed using thermogravimetric analysis (TG, DTG), differential thermal analysis (DTA), thermomechanical analysis (TMA), X-ray diffractometry, IR spectrophotometry and inductively coupled plasma spectroscopy (ICP).

Analyses were aimed in particular to determine the most striking aspect of the finds, the difference in colour between the outer surface (reddish) and the darker inner portion of several of the specimens. The other main points investigated and discussed are related to the firing temperature and chemical and mineralogical composition, of terracotta specimens.

Keywords: infra-red spectroscopy, plasma emission (ICP), prehistoric terracottas, thermal analysis, X-ray diffractometry

Introduction

The study of ancient terracotta finds is of considerable archaeological interest as they represent one of the earliest artefacts produced by man. Their complete characterization can thus provide information concerning the technological, artistic and cultural level reached by the population of a geographical site in historical and even prehistoric times.

The results presented herein stem from physico-chemical analyses performed by different techniques on five terracotta specimens from an archaeological dig on the Libyan Tadrart Acacus massif. The material, presumably potsherds, with impressed decoration obtained using double-pointed comb-like instruments, probably dates back to between 5000 B.C. and 8000 B.C. [l].

The present research was aimed at: the complete physico-chemical characterization of the terracottas studied; investigation of the firing temperature of the fragments; identification of the cause of the different colouring taken on by the various outer or inner portions of most of these terracottas.

* Author for correspondence: E-mail: mauro.tomassetti@uniroma1.it

1388–6150/2003/ $ 20.00
Akadémiai Kiadó, Budapest

The tests were performed using thermogravimetric analysis (TG), differential thermal analysis (DTA), thermomechanical analysis (TMA), X-ray diffraction (XRD), porosimetry, plasma emission spectroscopy (ICP), Fourier transform infrared spectroscopy (FTIR) and conventional microchemical techniques.

Among the analytical methods used in the present research, thermoanalysis and, in particular, three of the most important techniques related to it (TG, DTA and TMA) had a high analytical and guiding relevance. Moreover the importance of thermoanalysis' potential contribution to the characterization of many archaeological finds has been fully documented by researchers such as Wiedemann [2, 3], Odlyha *et al.* [4, 5] and Lamprecht [6]. More specifically, of the numerous works concerning the study of terracottas of different ages, carried out using mainly thermoanalytical methods suffice it to mention those of Mejdahl [7], Moropoulou *et al.* [8], Enriquez *et al.* [9] and Edwards *et al.* [10]. Furthermore, we deem to be of fundamental significance in this sector the thermodilatometric work done by Kiefer [11], Tite [12] and Roberts [13] on the determination of the firing temperature of ancient ceramics. This is an important problem as firing temperature depends above all on the characteristics of the kiln used, which to some extent reflect the technological level reached by the people making the products. For this reason, the study of terracotta firing temperature has been addressed by a number of workers, also using porosimetric (Morariu *et al.* [14]), thermal (Maggetti [15]) and more recently spectroscopic (Eiland and Williams [16] or Mirti [17]) methods. There is no doubt, however, that the thermodilatometric method as proposed and applied by the above-mentioned authors, together with the thermoanalytical observations, despite its drawbacks, perhaps represents the best known and most widely used method of those currently available. Also the present authors in recent years published some papers concerning the characterisation of ancient fictile statues and the values of their equivalent firing temperatures [18–20], or the analysis of wood finds [21–23] using thermal analysis.

Experimental

Sampling, apparatus and methods

The five terracotta finds examined, denoted for the purposes of this paper with the capital letters A→E (Fig. l), were found during an excavation campaign carried out within the framework of a convention with La Sapienza University of Rome and ENEA [1], and come from an archaeological dig on the Libyan Tadrart Acacus massif known as the 'Uan Telocat' shelter, and all probably belong to pastoral period pottery and dating to between 5000 and 8000 B.C. [1]. The five specimens were first carefully ground up into a homogeneous powder to be used in the various analyses, except for porosimetric analysis, for which tiny fragments of the specimens not subjected to any pretreatment were used directly as they were sufficiently clean and bore no traces of soil.

The thermogravimetric and differential thermal analyses were performed using a Du Pont apparatus (951 Thermogravimetric analyzer and DTA cell) coupled to a Thermal Analyst 2000 Du Pont system. The experiments were carried out at a heating rate of

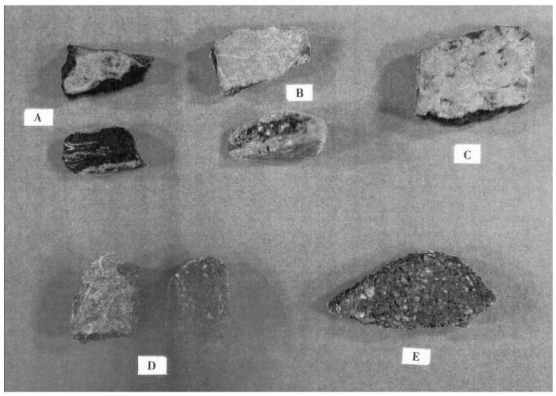

Fig. 1 Specimens of prehistoric terracottas from the Libyan Tadrart Acacus examined. Samples A, B, C, D, E

10°C min^{-1}, in static air. The thermomechanical tests were performed on a Mettler TMA 40 thermomechanical analyzer equipped with a cylindrical alumina specimen-holder (5 mm in diameter and 5 mm high) and an alumina piston, coupled with a TC 10 A microprocessor and a Swiss matrix printer. As well as recording the thermodilatometric curve, the specimen was placed in the cylindrical holder and subjected to an isothermal recompaction process at 25°C achieved by applying both a constant load of 0.4 N for 10 min on the piston together with a dynamic charge of 0.1 N (at a frequency of 5 cycles min^{-1}), as described in detail in a precedent paper [19]. At the end of this treatment the specimen was subjected to thermodilatometric scanning, between 25 and 1000°C, in the same cylinder, at a heating rate of 8°C min^{-1}, in static air conditions and with a constant applied load of 0.05 N.

X-ray diffraction tests were performed on an Isodebyflex PAD IIIA Seifert Automatic Powder Diffractometer using CuK_α radiation (λ=1.54 Å).

IR spectroscopic analyses were carried out using a Perkin Elmer mod. 1600 series FTIR infrared spectrophotometer, with direct dispersion of the powdered specimen in KBr pellets.

The analysis of chemical elements contained in the specimens was performed by an I.C.P., Jobin-Yvon, Type III- Sequential plasma emission spectrometer. The solution to be analyzed was obtained by mixing 200 mg of the ground specimen with 1.0 g of lithium tetraborate in a graphite crucible and by heating in an oven to 1000°C for 40 min after stirring at about 700°C. The pearl was cooled and then dissolved in 250 mL of aqueous solution containing 4 mL of HNO_3 (65 mass/mass %) and 4 mL of HCl (37 mass/mass %), stirring for 5 h. Tests to evaluate pore size distribution in the specimens were performed using a series 200 Carlo Erba mercury porosimeter.

Lastly, several classical chemical assays were performed on the specimens, mainly for the purpose of detecting the presence of iron(II) and iron(III) using classical wet way chemical methods of semimicro-qualitative analysis [24].

Results

Figure 1 shows the five fragments analysed. Of these, fragments A and B were subdivided into two parts so as to be able to photograph both the brick red coloured outer part and the black coloured internal part. Figure 2 shows the TG and DTG curves, between 30 and 1000°C, for the five specimens tested. Figures 3 and 4 show the TG and DTG curves referring to specimens B and D, again between 30 and 1000°C, respectively for the outer surface and the inner portion of the specimens; also the thermogravimetric curve of specimen D after reheating to 700°C is shown in Fig. 4.

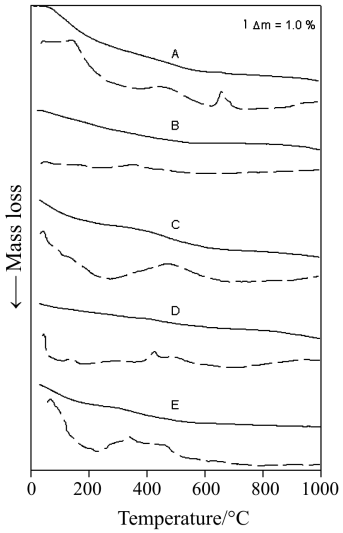

Fig. 2 Thermogravimetric curves (TG (——) and DTG (– – –)) for the five terracotta specimens (A, B, C, D, E) examined, obtained in static air conditions. Analysed samples were taken both from the outer surface and the inner portion of each specimen

The relevant thermogravimetric data, referring to the temperatures of the various steps and the loss of mass during the steps themselves, are summarized in Tables 1–3.

Temperatures were corrected for thermocouple non-linearity and are, of course, procedural temperatures [25]. Figures 5 and 6 show the DTA curves between 30 and 1000°C for whole specimens and for the outer surface, or the inner portion of some of the specimens, respectively. Figure 7 shows typical TMA and DTMA curves between 25 and 1000°C for specimens B, D and E. The X-ray diffraction spectra of the five specimens are shown in Fig. 8. Figure 9 shows typical X-ray diffraction spectra for the outer and the inner portion of the specimens B and D; the same figure also shows the X-ray diffraction spectrum of specimen D after it was heated to 1000°C. The main minerals contained in the five terracotta specimens and identified using this technique are indicated in the captions of the last two figures. Typical FTIR spectra for some of the specimens are

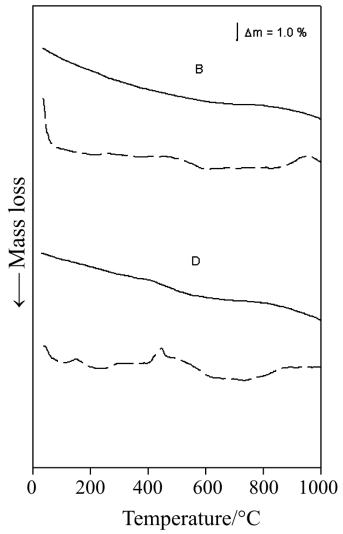

Fig. 3 Thermogravimetric curves (TG (——) and DTG (– – –)) of the two terracotta specimens B and D obtained in static air conditions. Analysed samples were taken exclusively from the outer portion of the two specimens B and D

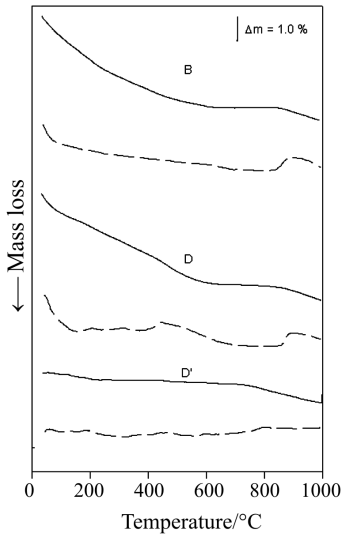

Fig. 4 Thermogravimetric curves (TG (——) and DTG (– – –)) of the two terracotta specimens B and D obtained in static air conditions. Analysed samples were taken exclusively from the inner portion of the two specimens B and D. (D'): TG (——) and DTG (– – –) curves performed exclusively on the inner portion of specimen D, but after previously reheating the specimens to 700°C

Table 1 Main thermogravimetric data of the five terracotta samples belonging to the Tadrart Acacus Libicus. Analysed samples are relative to the total (e.g. internal + external part of each find). TG in static air; heating rate 10°C min^{-1}

Sample	First step		Second step		Third step		Residue /% at 1000°C
	loss/%	pdt	loss/%	pdt	loss/%	pdt	
A	5.5	30 250	1.95	250 550	0.3	640 685	90.6
B	1.9	30 250	1.2	250 550	–	–	95.3
C	1.8	69 144	2.3	250 600	–	–	92.7
D	0.5	30 120	1.6	130 510	–	–	95.8
E	2.1	40 146	1.8	250 500	–	–	94.9

pdt = procedural decomposition temperature (°C): initial and final temperature of the step

Table 2 Main thermogravimetric data of the external parts of four terracotta samples belonging to the Tadrart Acacus Libicus. TG in static air; heating rate 10°C min^{-1}

Sample	First step		Second step		Residue /% at 1000°C
	loss/%	pdt	loss/%	pdt	
A(e)	6.0	30 250	1.9	250 520	91.0
B(e)	1.7	30 220	1.1	220 570	96.0
C(e)	3.4	30 250	2.2	250 560	93.0
D(e)	1.1	30 200	1.3	250 570	96.6

pdt = procedural decomposition temperature (°C): initial and final temperature of the step
(e) = external part of the sample

set out in Fig. 10. Table 4 shows the relative percentage of oxides of the main chemical elements contained in the five terracotta specimens, as determined by plasma emission spectroscopy. Lastly, in Fig. 11, typical porosimetric curves show the cumulative percentage of the pore volume *vs.* the pore radii, for specimens A and C.

Discussion

The macroscopic observation of the 5 specimens analysed indicates that the paste was fairly compact in the case of specimens A–D but not for specimen E.

Table 3 Main thermogravimetric data of the internal parts of four terracotta samples belonging to the Tadrart Acacus Libicus. TG in static air; heating rate 10°C min^{-1}

Sample	First step		Second step		Residue /% at 1000°C
	loss/%	pdt	loss/%	pdt	
A(i)	4.5	30–187	2.0	250–535	90.0
B(i)	2.1	30–190	1.3	250–600	92.3
C(i)	–	–	2.4	250–550	91.7
D(i)	1.3	30–170	1.8	250–600	92.1

pdt = procedural decomposition temperature (°C): initial and final temperature of the step. (i) = internal part of the sample

Table 4 Relative percentage of oxides of the five terracotta samples belonging to the Tadrart Acacus Libicus; analysed samples are relative to the 'total' (i.e. internal+external) part of each find (A→E)

Oxide	A	B	C	D	E
CaO	1.73	0.93	1.24	1.68	15.30
Al_2O_3	16.97	22.94	19.44	26.02	19.76
Fe_2O_3	12.40	8.82	8.85	7.88	9.94
SiO_2	67.53	65.97	68.30	62.67	50.00
MnO_2	0.12	0.02	0.06	0.07	0.11
MgO	0.46	0.48	0.80	0.88	4.04
TiO_2	0.71	0.75	1.18	0.61	0.74
BaO	0.00	0.00	0.04	0.10	0.00
PbO	0.03	0.00	0.01	0.01	0.02
SrO	0.02	0.01	0.02	0.02	0.03
ZnO	0.02	0.02	0.03	0.02	0.05
ZrO_2	0.01	0.04	0.02	0.04	0.01
Y_2O_3	0.00	0.01	0.01	0.01	0.00

% values of each oxide were calculated on the basis of the content of respective metal in the finds, experimentally determined using plasma emission (ICP) spectrometry and taking into account of the reported stoichiometric formula for each oxide

Furthermore, particularly in specimens A, B and C a difference in the colouring is observed between the reddish coloured outer surface and the darker inner core. On the other hand, specimen E, is dark-coloured throughout and it seems to consist of a coarser and more friable paste; it is so different from the other specimens that a much more primitive method of firing than the other specimens, perhaps even simple sun drying, is suggested.

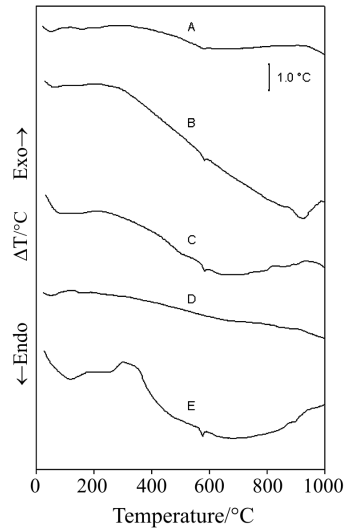

Fig. 5 DTA curves of the five terracotta specimens examined, obtained in static air conditions. Analysed samples taken from both the inner portion and the outer part of each specimen

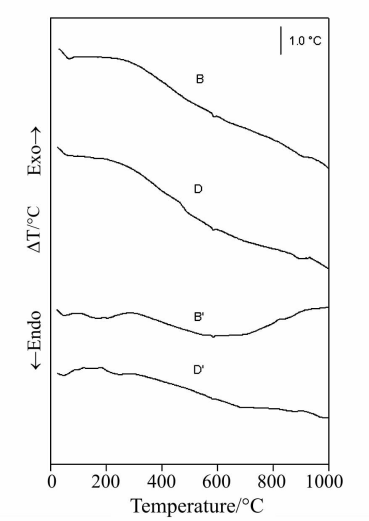

Fig. 6 DTA curves for terracotta specimens B and D, obtained in static air conditions. Curves (B) and (D): DTA curves for samples A and D. Analysed samples taken exclusively from the outer portion of specimens B and D. Curves (B') and (D'): DTA curves for samples B and D. Analysed samples taken exclusively from the inner portion of specimens B and D

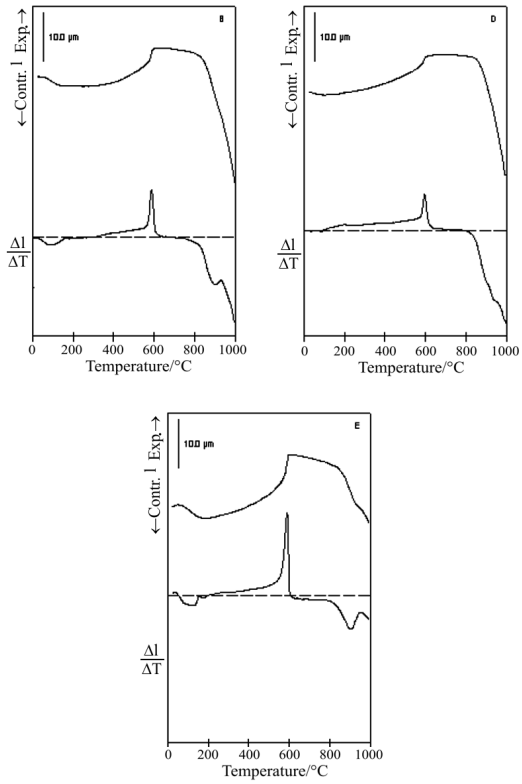

Fig. 7 Thermomechanical curves (TMA and DTMA) for terracotta specimens B, D and E, obtained in static air conditions. In each frame TMA is the upper curve and DTMA is the lower curve. Analysed samples were taken both from the outer portion and the inner portion of each specimen

Analysis of the FTIR spectra (Fig. 10), in which the silicate bands are clearly visible [26], led us to postulate the presence of residues in these terracotta specimens of the clays used to make these artefacts. This was confirmed by X-ray diffraction (Fig. 8), which allowed traces of clay minerals such as illite and muscovite to be identified.

When the analysis was replicated using X-ray diffraction on a specimen previously heated to 1000°C, a decrease was observed in the intensity of the diffractometric peaks referring to these silicates or indeed to the disappearance of several of them (Fig. 9). Lastly, the DTA curves (Figs 5 and 6) often display a large endothermic gap between about 350 and 600°C, a zone characterized by the loss of the water of constitution, which occurs during the process. The process is accompanied by a loss of hydroxyl groups of the clay-like minerals such as illite, montmorillonite and muscovite.

Furthermore, the loss of –OH groups is known to lead to irreversible changes in the crystalline structure of these minerals [27]; therefore the changes in the crystalline structure of the illite silicates probably give rise to the slightly expansive process

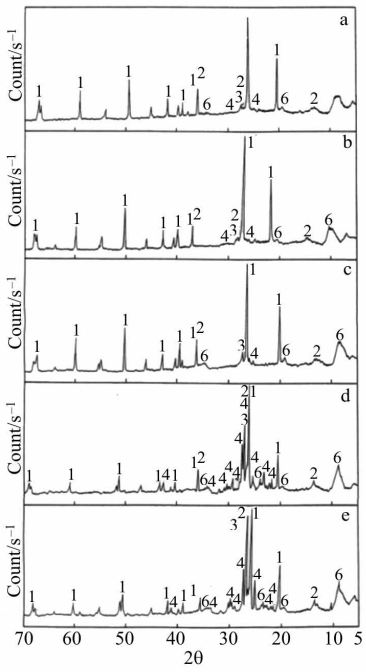

Fig. 8 X-ray diffraction spectra of the five terracotta (A, B, C, D, E) specimens examined. Analysed samples were taken both from the outer portion and the inner portion of each specimen. 1. Quartz; 2. γ-FeO(OH); 3. Feldspar; 4. Plagioclase; 6. Illite

observed in the TMA and DTMA curves in Fig. 7 that begins at about 300 and ends at about 530°C [12], immediately preceding the extensive expansive process occurring between 530 and about 650°C attributed to the allotropic transformation of quartz from the α to the β form [19, 28]. The presence of these clay residues has warranted the hypothesis that the terracottas were not subjected to a satisfactory firing process, i.e. their firing temperature never exceeded 600–650°C. Further confirmation of this was obtained by repeating the DTA testing of specimens after heating the specimens themselves to 700°C for 50 min; in the latter case it was found that the endothermic gap described above disappeared. Likewise, the TG curve of the inner part of specimen D, which had previously been heated for 50 min at 700°C, showed no perceptible mass loss over the range 350–600°C; this loss was however visible in the TG curve of the unheated specimen (compare curves D and D' in Fig. 4).

However, it was observed [29] that, when fired at temperatures below 800°C, clay artefacts can gradually regain at least part of the interleaf water as well as, although more slowly, the water of constitution. Mejdahl [7] showed that the absence of a clear-cut endothemic peak at 550°C in the DTA curves, which is indicative of loss of water of constitution in clay minerals, points to a firing temperature of over

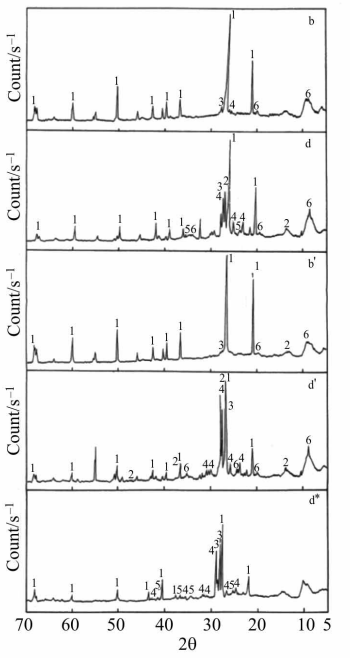

Fig. 9 X-ray diffraction spectra of the two terracotta specimens B and D. Curves (B) and (D): Diffraction spectra referring to samples taken exclusively from the outer portion of the two samples B and D. Curves (B') and (D'): Diffraction spectra referring to samples taken exclusively from the inner portion of the two samples B and D. Curves (D*): Diffraction spectra referring to samples taken exclusively from the inner portion of sample D, but carried out after reheating the specimen to 1000°C in a current of air. 1. Quartz; 2. γ-FeO(OH); 3. Feldspar; 4. Plagioclase; 5. Hematite; 6. Illite

400–450°C at least. As in our case there is actually no well-defined peak around 550°C, and on the contrary we find a wide endothermic gap, it is reasonable to assume that a rehydration process has been triggered, which is the cause of the large endothermic gap observed in the DTA curve. On the strength of the latter considerations, the firing temperature would certainly lie in the range of 450–800°C. Furthermore, taking into account also the previous observations, concerning the presence of clay residues, this range could probably be reduced to 450–650°C.

On the other hand, the analysis of the relative thermodilatometric plots obtained via TMA (Fig. 7) performed on the basis of the criteria suggested by Tite [12], leads to the conclusion that the firing temperature for specimens A, B, C and D is in the vicinity of 650°C, which is in fair agreement with the estimated range based on the observations reported above and indicated by other thermal analysis techniques.

In the case of specimen E, the TMA curve indicated a firing temperature of about 600°C, i.e. at least 50°C lower than for the other specimens. However, it should

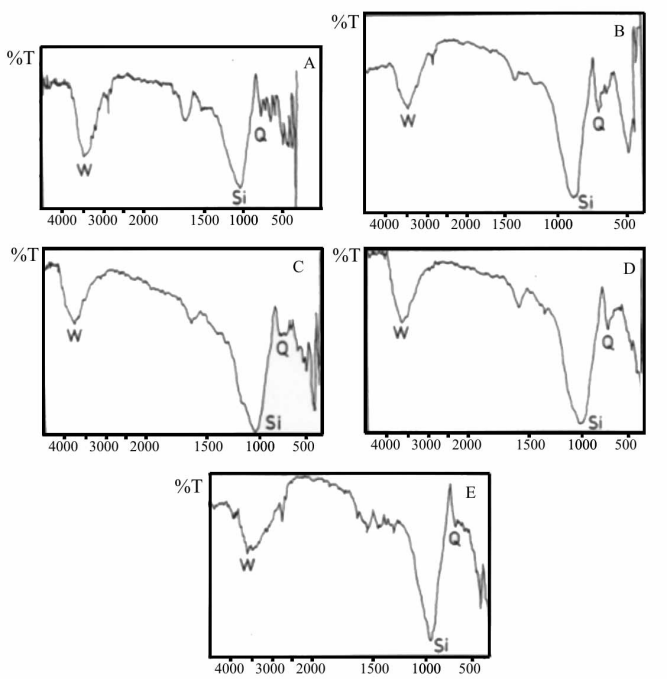

Fig. 10 FTIR spectra of the five terracotta specimens examined (A, B, C, D, E): W = water; Si = silicates; Q = quartz

be borne in mind that no mathematical corrections [12] were made to the estimated firing temperature found using this method. Finally, the typical porosimetric curves reported in Fig. 11 show that the pore structure of the specimens is relatively dishomogeneous, which is indeed typical of clays fired at comparatively low temperatures [14]. This therefore supports the estimated value of about 600–650°C for the firing temperature obtained from TMA analysis.

The thermogravimetric analysis, as it emerges from the data in Tables 1–3, in addition to the process observed at temperatures of around 250–600°C and to be ascribed as we have seen not only to the loss of both residual interleaf water and water of constitution, also displays a lower temperature step (30–200°C), in which also the uncombined water contained in the specimen is lost.

At higher temperatures (650–700°C), and in practice only in the case of specimen A, also a small step may be observed which is due to the decomposition of carbonate traces [19]. Lastly, Tables l–3 show also the percentage thermogravimetric residues at 1000°C for both whole specimens and those referring solely to the inner or the outer part of the specimens themselves. The histogram in Fig. 12a shows the percentage of thermogravimetric residues at 1000°C. It is apparent that the following trend is always the same: the residue at 1000°C of the outer parts of the specimen is always slightly greater than the whole (outer part plus inner part) for each specimen. In its turn the latter is greater than

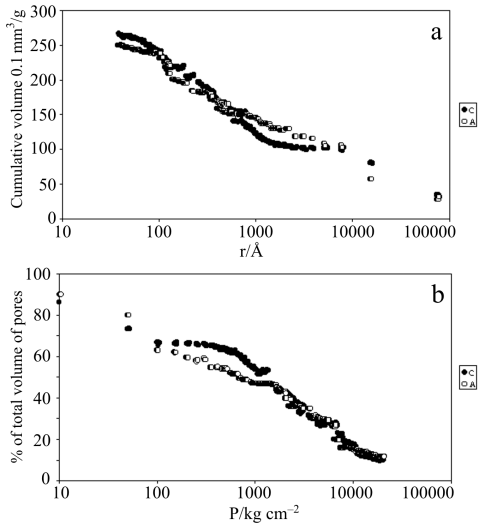

Fig. 11 a – Porosimetric curves of the two terracotta specimens A and C showing the cumulative percentage of the pore volume *vs.* the pore radii, b – Partition functions

that one of the inner parts of the specimen alone. This trend is always observed even when the differences are actually only small, even of the same order as of instrumental error. Also the data shown in Fig. 12b are significant. Here the histogram shows the percentage loss of mass for the outer and inner parts of the specimens examined, as recorded in the thermogravimetric step located at about 250–600°C; as we have seen, it is here that the interleaf water and water of constitution are lost. Also in this case the differences are very slight. Nevertheless, the loss observed in the case of the inner parts of the specimens is slightly greater than that recorded for the outer parts. These observations thus seem to support what even macroscopic observation of the different appearance of the outer parts vis-à-vis the inner parts of specimens A+D seems to suggest, i.e. that the outer surface of the specimens attains a higher firing temperature than the inner part. This temperature difference, although hard to be quantified, is very probably the cause of the colour difference observed between the outer part and the inner part, above all in the case of specimens A, B and C.

At the outset, a number of different hypotheses were proposed to account for the dark colouring of the inner part of several fragments. These hypotheses took into account also the information reported by other authors who had to cope with archaeological problems of the same type:

1. Firing in a reducing atmosphere [27] with consequent presence in the specimen of:
a) carbon (as in the classical case of the Etruscan bucchero) [30],
b) dark-coloured Fe(II) oxides [30].
2. The presence of non-negligible quantities of manganese oxide (pyrolusite) [31].

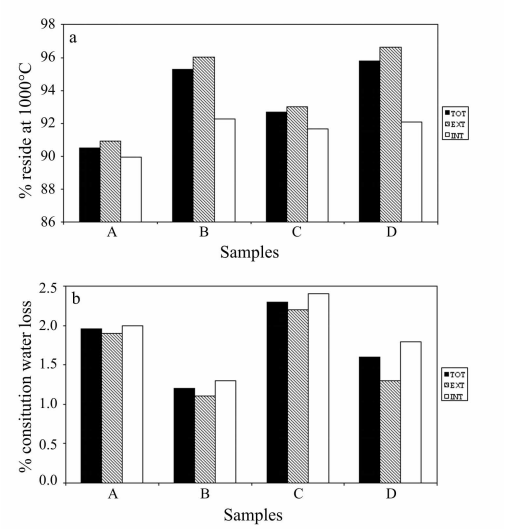

Fig. 12 Histograms: a – of the thermogravimetric residues at 1000°C , b – of the mass loss at the second TG step, of the terracotta specimens A, B, C and D, referring exclusively to the outer portion, and to the inner portion of samples, as well as to whole (outer + inner) parts of the respective specimens

As far as the possible presence of significant quantities of carbon and Fe(II) oxides produced in the specimen subjected to a reducing atmosphere in the kiln is concerned, no evidence was found in the DTA plots (Fig. 6) carried out in oxidant atmosphere (i.e. air) of the specimen of any exothermic process due to the oxidation of carbon or fossil carbonaceous material [30], nor even of any process of Fe(II) oxidation [30]. Furthermore, the diffractograms recorded for the inner part of the fragments show no evidence of the presence of Fe(II) oxides (Figs 8 and 9). This result, which is confirmed also by wet-way chemical microanalysis [24], allows us to reject the hypothesis of the formation of a dark core due to firing in a strongly reducing atmosphere that would have presumably produced dark-coloured carbonaceous material or Fe(II) oxides. Moreover, in the diffractograms shown in Figs 8 and 9 no peak can be ascribed to pyrolusite; moreover, the data set out in Table 4 referring to the ICP analysis of our specimens indicates that the quantity of manganese present in the fictile specimens is in any case not large enough to account for such a conspicuous dark colouring of the specimens [31]. It thus seems more reasonable to attribute the dark colouring to the presence of a dark coloured Fe(III) hydrated oxide, probably lepidocrocite (γ-FeO(OH)) [32] in the inner part of the specimens A–D, whose presence in the specimen was confirmed by the X-ray diffraction spectra shown in Figs 8 and 9. Furthermore, by heating the inner part of a specimen to a temperature of about 1000°C, and then recording again the diffractometric peak on it, there is (Fig. 9) a clear-cut decrease (and practically the disappearance) of the lepidocrocite peaks accompanied by the appearance of hematite (Fe_2O_3) peaks (curve D* in Fig. 9). The ob-

servation is also supported by the recent work of Balek and Subrt [33], who claims that if lepidocrocite is subjected to a process of thermic dehydration α-Fe_2O_3 is actually formed which is initially pseudo-amorphous and subsequently, as the temperature increases, becomes increasingly crystalline. A process of this type would also account for the relatively small quantity of hematite in any case detected by X-ray diffraction, also on the outer surface of the fragments. If in fact during firing the artefact did not reach a sufficiently high temperature that was maintained for long enough to transform the lepidocrocite into crystalline hematite, we would be dealing with a pseudo-amorphous form that would be hard to be detected by X-ray. Moreover, this would all be compatible with a comparatively low firing temperature, as it was already indicated in the other experimental data reported in the present paper. Indirect confirmation of the presence of lepidocrocite comes also from the FTIR analysis carried out on the dark core of the specimen after reheating to 500°C. Indeed, after reheating, the IR spectrum of the specimen shows that the broad band to be ascribed to the stretching of the –OH group of the water at about 4300 cm^{-1} (Fig. 10) does not disappear completely, as it would be expected if only due to moisture and to the water associated with clay-like minerals. The partial reduction observed in this band can be attributed, at least in part, to the presence of hydrogen bonds formed between the Fe(III) oxides and hydroxides contained in the specimens [34].

Lastly, an analysis of the ICP data contained in Table 4 indicates a high degree of homogeneity of all the chemical components of specimens A, B, C, and D. In the case of specimen E, in addition to the difference in appearance and firing temperature, a considerable difference was found also in the chemical composition compared with that one of the other four specimens. This difference is particularly apparent in the case of the percentages of calcium and magnesium present, which are much higher in specimen E than in the other examined specimens. All this would seem to indicate that specimen E represents a different type of production or that different raw materials and technologies were applied than in the case of the other four analysed specimens.

* * *

We wish to thank Dr. R. Ponti of the Cattedra di Etnografia Preistorica dell'Africa of University of Rome La Sapienza for making available the specimens and for his precious collaboration.
This work was financially supported by National Research Council (CNR) or Italy Targeted Project MADESS.

References

1 G. Aurisicchio and G. F. Guidi, Arte e cultura del Sahara preistorico, M. Lupacciolu (Ed.), Quasar (Publ.), 1992 p. 63.
2 H. G. Wiedemann, Thermochim. Acta, 148 (1989) 95.
3 H. G. Wiedemann, Thermochim. Acta, 229 (1993) 215.
4 M. Odlyha and C. F. Simpson, J. Therm. Anal., 38 (1992) 361.
5 M. Odlyha and A. Burmester, J. Therm. Anal., 33 (1988) 1041.
6 I. Lamprecht, Thermochim. Acta, 234 (1994) 179.

7 V. Mejdahl, Archaeometry, 22 (1980) 197.
8 A. Moropoulou, A. Bakolas and K. Bisbikou, Thermochim. Acta, 2570 (1995) 743.
9 C. R. Enriquez, J. Danon and M. Da C. M. C. Beltrão, Archaeometry, 21 (1979) 183.
10 W. I. Edwards and E. R. Segnit, Archaeometry, 26 (1984) 69.
11 C. Kiefer, Bull. Soc. Franc. Ceram., 35 (1957) 95.
12 M. S. Tite, Archaeometry, 11 (1969) 131.
13 J. P. Roberts, Archaeometry, 6 (1963) 21.
14 V. V. Morariu, M. Baydan and I. Ardelean, Archaeometry, l9 (1977) 187.
15 M. Maggetti, in: Archaeological Ceramics, J. S. Olin and A. D. Franklin Eds, Washington: Smithsonian Institution 1982, pp. 121–133.
16 M. L. Eiland and Q. Williams, J. Arch. Science, 27 (2000) 993.
17 P. Mirti, Archaeometry, 40 (1998) 45.
18 M. Tomassetti, L. Campanella, P. Flamini and G. Bandini, Thermochim. Acta, 291 (1997) 117.
19 L. Campanella, G. Bandini, P. Flamini and M. Tomassetti, Sci. Technol. Cult. Heritage, 3 (1994) 169.
20 L. Campanella, P. Flamini and M. Tomassetti, in: The Ceramics Cultural Heritage, P. Vincenzini Ed., Techna Srl., Faenza, Italy 1995, p. 287.
21 M. Tomassetti, L. Campanella, R. Tomellini and C. Meucci, Thermochim. Acta, 117 (1987) 297.
22 M. Tomassetti, L. Campanella and R. Tomellini, Thermochim. Acta, 170 (1990) 51.
23 L. Campanella, M. Tomassetti and R. Tomellini, J. Therm. Anal., 37 (1991) 1923.
24 G. Charlot, Analisi chimica qualitativa, Piccin, Milan 1977.
25 U. Biader Ceipidor, G. D'Ascenzo, M. Tomassetti and E. Cardarelli, Thermochim. Acta, 30 (1979) 15.
26 J. M. Hunt and D. S. Turner, Anal. Chem., 8 (1953) 1169.
27 N. Cuomo di Caprio, La ceramica in archeologia, L'Erma, Bretschneider 1988.
28 B. Fabbri and C. Fiori, in: Caratterizzazione e reattività di materiali speciali, AICAT-IRTEC (CNR), Faenza, Italy 1990 p. 107.
29 R. E. Grimm, Clay Mineralogy, McGraw Hill, 1968, p. 314.
30 A. Flamini, G. Graziani, O. Grubessi and P. Lorenzo, Gea Archaeologia, l/2 (1977) 7.
31 V. Francaviglia, M. E. Minardi and A. Palmieri, Archaeometry, 17 (1975) 223.
32 A. R. Dinesen, C. T. Pedersen and C. Bender Koch, J. Therm. Anal. Cal., 64 (2001) 1303.
33 V. Balek and J. Subrt, in: Abstract Book of 6th European Symposium on Thermal Analysis and Calorimetry, Grado, Italy 1994, p. 26.
34 B. Siesmayer, A. Giebelhausen, J. Zambelli and J. Riederer, Z. Anal. Chem., 277 (1975) 193.